Formation of Carbon Clusters in the Initial Stage of Chemical Vapor Deposition Graphene Growth on Ni(111) Surface

ARTICLE *in* THE JOURNAL OF PHYSICAL CHEMISTRY C · SEPTEMBER 2011

Impact Factor: 4.77 · DOI: 10.1021/jp2051454

5 AUTHORS, INCLUDING:

Junfeng Gao
Institute Of High Performance Computing
32 PUBLICATIONS **669** CITATIONS
SEE PROFILE

Hong Hu
The Hong Kong Polytechnic University
143 PUBLICATIONS **1,105** CITATIONS
SEE PROFILE

Jijun Zhao
Dalian University of Technology
390 PUBLICATIONS **8,255** CITATIONS
SEE PROFILE

Feng Ding
The Hong Kong Polytechnic University
123 PUBLICATIONS **2,968** CITATIONS
SEE PROFILE

THE JOURNAL OF PHYSICAL CHEMISTRY C

ARTICLE

pubs.acs.org/JPCC

Formation of Carbon Clusters in the Initial Stage of Chemical Vapor Deposition Graphene Growth on Ni(111) Surface

Junfeng Gao,[†,‡,∥] Qinghong Yuan,[†,∥] Hong Hu,[†] Jijun Zhao,[*,‡] and Feng Ding[*,†,§]

[†]Institute of Textiles and Clothing, Hong Kong Polytechnic University, Hong Kong, China

[‡]Key Laboratory of Materials Modification by Laser, Ion and Electron Beams, Dalian University of Technology, Ministry of Education, Dalian 116024, China

[§]Department of ME&MS, Rice University, Houston, Texas 77005, United States

Supporting Information

ABSTRACT: To understand the nucleation of carbon atoms to form graphene on transition metal substrates during chemical vapor deposition (CVD) synthesis, carbon clusters supported on Ni(111) surfaces, namely C_N@Ni(111) (where $N \leq 24$), were explored systematically using density functional theory (DFT) calculations. Very different from the freestanding C clusters, on a Ni(111) surface, the C chain configuration is superior to the C ring formation and dominates the ground state until $N > 12$. A ground state structural transition from a one-dimensional C chain to a two-dimensional sp^2 network (or graphene island) occurs at $N = 12$. It is surprising that incorporating one to three 5-membered-rings (5MRs) or pentagons into a graphene island is required to achieve the energetically most stable structure. This deep insight into the supported C cluster formation is crucial for understanding the growth mechanism of graphene on a transition metal surfaces in CVD experiments and the experimental design of CVD graphene growth.

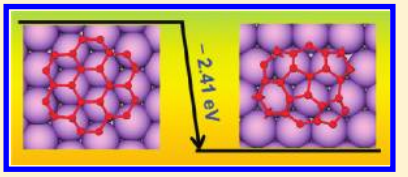

Nowadays, graphene is a superstar material in many fields including material science, physics, chemistry, electronics, and biology.[1−3] In addition to the high Young's modulus, strength and thermal conductivity that are comparable to those of carbon nanotubes (CNTs),[4−6] it possess a largely extended two-dimensional (2D) area and distinctive electronic properties.[7,8] Its superior mechanical, thermal, electronic, optical, and chemical properties ensure numerous applications in composites, renewable energy generation and storage, chemical sensors, catalysts, etc. In particular, graphene is believed to be the most promising candidate for replacing silicon in future electronic applications.[9−11]

In order to realize these extraordinary applications, growing high quality graphene in large areas and in macroscopic quantities is highly desirable. Currently, the established methods of synthesizing graphene include mechanical peeling,[1,12] high temperature sublimation of SiC,[13−16] intercalation or functionalization of graphite,[17,18] and transition metal (TM) catalyzed chemical vapor deposition (CVD) growth.[19−31] Among these methods, the CVD growth on TM surfaces is most promising for synthesizing high quality and large area graphene at relatively low cost.

Similar to the synthesis of carbon nanotubes, the CVD growth mechanism can be understood by a vapor−liquid−solid (VLS) or vapor−solid−solid (VSS) model.[32−35] In a CVD experiment, a complete process of graphene growth includes three relatively independent stages: (i) the initial stage, (ii) the graphene nucleation stage, and (iii) the continuous extension of graphene islands to cover the whole metal surface.

In stage (i), the C precursor molecules (e.g., CH_4, C_2H_2, and C_6H_6) dissociate on the TM surface, forming C monomers or dimers by dehydrogenation. For a TM which has stable carbide phases (e.g., Ni, Fe, Co, Mo, ...), the C atoms may dissolve into the TM bulk at high temperature and these dissolved C atoms may segregate and precipitate to form graphene layers on the TM surface upon cooling. For a TM which has no carbide phase (e.g., Cu, Au, ...), these dissociated C atoms stay on the surface only.

Once the concentration of C monomers or dimers on a TM surface reaches a critical value, the nucleation of graphene, namely, stage (ii) starts. During this stage, the C monomers or dimers aggregate to form small C clusters of various sizes, but most of these clusters are metastable and will dissociate back into monomers or dimers again. Once the carbon cluster size exceeds a critical size, which is determined by the conditions of growth (e.g., temperature, pressure of precursor gas, interaction between C and TM), stage (iii) starts.

By continuously adsorbing C monomers, dimers, or small clusters around it, a matured C cluster (whose size is bigger than the critical nucleation size) will keep growing into a large graphene island. As a consequence of Ostwald ripening, the continuous adsorption of small C clusters will lead to a reduction of C concentration in the nearby region; thus, it destabilizes the smaller graphene islands. The density of stable graphene islands on a catalyst surface is determined by the C concentration in the nucleation stage (ii). Once these stable islands grow large enough, their edges will meet and coalesce on the catalyst surface. The coalescence of two large graphene islands with different lattice orientations must then result in the formation of grain boundary, which is the most important type of defect in CVD graphenes.[36,37]

Received: June 1, 2011
Revised: July 31, 2011
Published: August 11, 2011

Among the above-mentioned three stages, stage (ii), the nucleation of graphene, is crucial for the following reasons. First, the nucleus size and nucleation barrier determine the incubation time (the time required to form the first graphene island that is bigger than the critical nucleation size). Second, the nucleation barrier, nucleus size, C concentration, and diffusion barrier of C atoms on TM surface determine the density of graphene islands on metal surface. Since the merging of two graphene islands would normally lead to a grain boundary between them, it is critical for graphene quality control.

So far, there have been numerous experimental studies on the continuous growth of graphene, stage (iii), but investigations of stages (i) and (ii) are relatively rare because of the difficulty in observing very small C aggregates (e.g., C monomers, dimers, or clusters that contain a few tens of C atoms) on the TM surfaces. Recently, McCarty et al. investigated graphene nucleation on Ru(0001) or Ir(111) surfaces.[28,38,39] They observed the change of C monomer concentration during the aforementioned three stages and revealed a significant reduction of C concentration after the nucleation stage. Lacovig et al. have observed dome-like small C islands containing six-membered rings and demonstrated that C atoms on the edge of a graphene island interact strongly with the TM metal surface.[40]

From a theoretical viewpoint, Zhang and co-workers have studied the formation of C monomers and dimers on various TM terraces or near a step edge.[41] Saadi et al. have tried to explain the role of metal steps during graphene nucleation with a continuous model.[42] Using a tight-binding grand canonical Monte Carlo (GCMC) simulation, Hakim et al. have investigated the nucleation of graphene on a Ni(111) surface and discussed the role of transition metals during defect healing in graphene growth.[43,44] We have discussed in detail the role of metal step edge in graphene nucleation on transiton metal surface by DFT calculation recently.[45] However, there are still many unsolved or even untouched puzzles about the CVD growth of graphene. For instance, how does the TM surface affect the configuration of C clusters via passivation of the edge C atoms? What is the most stable form for a C cluster on a TM surface? What are the differences between free-standing C clusters (which have been comprehensively investigated to understand the formation mechanism of fullerenes) and TM-supported ones? Answering these questions is not only of fundamental interest but also crucial for achieving high quality graphene in CVD experiments. However, to the best of our knowledge, there have so far been no systematic explorations of the structures of C clusters on TM surfaces.

This paper aims to address the aforementioned issues. Using the Ni(111) surface as an example, we studied the TM-supported C clusters with one to twenty-four C atoms by means of ab initio calculations. We found that a C chain is very stable at small size and a transition to graphene islands occurs at a critical size of $N = 12$. Beyond this, sp^2 graphene islands consisting of one, two, or three pentagons are significantly more stable than those with only hexagons. These theoretical results provide very useful insights into the nucleation mechanisms of graphene, which may then be used to guide the experimental CVD synthesis of high-quality graphene.

METHODS

Ab initio calculations were performed by using the spin-polarized density functional theory (DFT) and plane wave pseudopotential technique, as implemented in the Vienna ab-initio simulation package (VASP).[46,47] Generalized gradient approximation (GGA) with the PW91 functional[48] was used to describe the exchange-correlation interaction. Ultrasoft pseudopotentials[49,50] were used to describe the core electrons. The plane-wave basis kinetic energy cutoff of 400 eV and convergence criterion of 10^{-4} eV were used in all calculations. The validity of using 400 eV as cutoff energy for C-TM system has been carefully justified by calculating the formation energy of C_1@Ni(111). The calculated formation energies of C_1@Ni(111) relative to free-standing graphene are 1.38 and 1.35 eV by using 400 and 600 eV as cutoff energies, respectively. Beyond, exact same cutoff energy has been used in previous studies of C-TM system.[40,42,51]

Ni is one of the most used catalysts for graphene CVD synthesis and it is very fortunate that Ni(111) surface matches the graphene lattice very well.[52] In this study, a bilayer slab model of Ni(111) surface with a fixed bottom layer was used. As shown in previous studies, inclusion of one more layer does not change the results significantly.[53] 20 Å unit cell length along the direction that is perpendicular to the slab surface is used to make sure that there's no interaction between unit cells. For C_1~C_{16}, models include chains, rings and networks, so Ni(111) slab unit cell were gradually expanded to make sure the distance between two neighboring C clusters was more than 9 Å. The Brillouin zone was also sampled by an individual K-point mesh as the size of C cluster grows. For C_{17}~C_{24}, only sp^2 network were considered and every unit cell contains (6×6) Ni(111) unit cells.

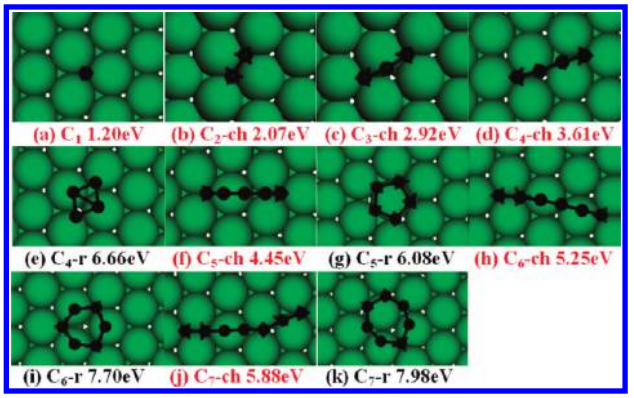

Figure 1. Structures and formation energies of C_1~C_7 clusters on a Ni(111) surface. "r" and "ch" in the notation C_N-r or C_N-ch stand for ring and chain, respectively. For each cluster size, the lowest-energy isomer is highlighted by red labels.

RESULTS

Very Small Carbon Clusters: C_1~C_7. Figure 1a–k presents the optimized configurations of very small C_N clusters with $N = 1$–7. In this size range, there are not enough C atoms to form a sp^2 island containing at least two connected polygonal rings; thus only C chains and C rings are considered. This is similar to the case of gas-phase clusters in vacuum.[54] In all these calculations, the formation energy of a given C cluster supported on Ni surface is defined as

$$E_F = E_{CN@Ni} - N^*\varepsilon_G - E_{Ni} \quad (1)$$

where $E_{CN@Ni}$ is the energy of the hybrid system, ε_G is the energy per atom of Ni(111) surface supported graphene, and E_{Ni} is the energy of the Ni substrate.

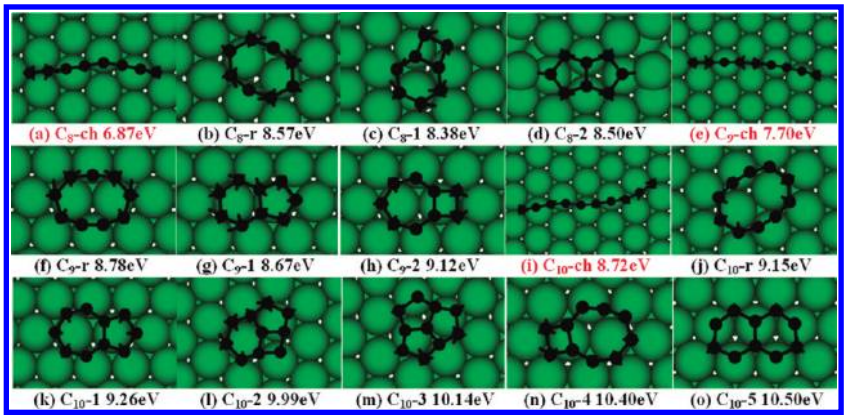

Figure 2. Structures and formation energies of C_8∼C_{10} isomers on a Ni(111) surface. "r" and "ch" in the notation C_N-r or C_N-ch stand for ring and chain, respectively. For each cluster size, the lowest-energy isomer is highlighted by red labels.

A single C atom on a hollow site of a Ni (111) surface has a small formation energy of 1.2 eV, which is about 1 order of magnitude lower than the formation energy of a single C atom in vacuum (8.4 eV calculated with the same method). On the Ni (111) surface, the binding energy of an individual C atom is 7.2 eV and the calculated C−Ni bond length is 1.77 Å, both in good agreement with previous work,[42] in which the formation energy of a C monomer is 1.25 eV.

The formation energy of a C_2 dimer is 2.07 eV, which is higher than that of a single C atom but less than the summation of two isolated C atoms. This implies that a carbon dimer on the Ni(111) surface is more stable than two monomers in the nucleation stage of graphene. The computed C−Ni bond length of 1.87 Å in C_2 dimer is slightly longer than that for the Ni-supported C monomer. The C−C distance in the supported dimer is 1.33 Å, which is a typical length of the C═C double bond. A C_3 triangle, the smallest possible ring formation, is unstable on the Ni (111) surface and transforms into a C_3 chain directly upon relaxation. C_4 has a metastable 4-membered-ring conformation, but its formation energy is 3.05 eV higher than that of chain isomer, implying that the C_4 ring is extremely unstable. Surprisingly, individual five-, six-, and seven-membered rings, which are the most populous polygons in graphene, fullerenes and CNTs, are significantly less stable than the corresponding C_5, C_6, and C_7 chains by 1.63, 2.45, and 2.1 eV, respectively. As we will demonstrate later, the two end atoms of a carbon chain bind to the hollow sites of the Ni(111) surface strongly and thus stabilize the chain configuration significantly. A carbon ring can be viewed as a bent chain without ends but carrying extra curvature energy. Considering the metal passivation of the end atoms in a chain and the large curvature energy in a small carbon ring, the ring configuration is less stable than the chain within the explored size range.

It is interesting to note that the formation energy of a carbon chain increases nearly linearly going from C_1 to C_7 with an increment of ∼0.8 eV per atom. This can be understood by their 1D structure. Hence, during the initial stage of graphene growth on the TM surface, a carbon chain of sufficient length should nucleate first. The nucleation of a carbon chain must be a typically 1D type of behavior, in which nucleation barrier G^* is a constant and appears at $N^* = 1$ (N^* is the size of the nucleus). Consistent with the present study, C chains have frequently been observed in previous MD and MC simulations of CNTs and graphene growth on metal clusters or surfaces.[43,55−57]

Small Carbon Clusters: C_8∼C_{10}. The geometrical structures and formation energies of C_8∼C_{10} isomers are shown in Figure 2. In this size range, small carbon islands or sp^2 C networks start to emerge. Surprisingly, the C chains (Figure 2, panels a, e, and i) are still energetically the most preferred.

As shown in Figure 2, all possible sp^2 isomers of C_8, C_9, and C_{10} have been explored, but their formation energies are all higher than those of the corresponding chain configurations. The energy difference between chain and the most stable sp^2 isomer reduces from 1.49 eV for C_8 to 0.97 eV for C_9, and further to 0.54 eV for C_{10}. Such a tendency indicates that the sp^2 network isomers (or small graphene islands) become more and more stable as the cluster size increases. As the cluster grows larger, a ground structure transformation from a C chain to an sp^2 network would occur inevitably. C_{10} has an isomer which consists of two six-membered-rings. Surprisingly, it possesses the highest formation energy among all isomers we have considered.

Medium-Sized Carbon Clusters: C_{11}∼C_{13}. Starting from C_{11}, the number of possible isomers of the sp^2 aggregates becomes larger and larger. Here only some important low-lying isomers are presented in Figure 3. The ground state of C_{11} is still a linear chain; but the energy difference between a chain and the most stable sp^2 isomer is very small (0.48 eV only). The ground structural transition from a C chain to an sp^2 isomer occurs at N = 12. The formation energy of the most stable C_{12} sp^2 network isomer, which is composed of two hexagons and one pentagon (6|6|5, Figure 3h), is lower than that of the C_{12} chain by 0.31 eV (Figure 3f). As the cluster grows larger, the stability of the sp^2 networks is further enhanced. For example, the formation energy of the most stable configuration for C_{13} (island of 6|5|5|5, Figure 3o) is 0.46 eV lower than that of the C_{13} chain (Figure 3m). C_{13} has a particular isomer which contains only three hexagons (6|6|6, Figure 3t). Again, its formation energy is ∼2 eV higher than that of the ground structure (Figure 3o).

Larger Carbon Clusters: C_{14}∼C_{24}. As the cluster size increases further, the energy difference between the chain and the most stable sp^2 aggregate becomes larger and larger (e.g., 0.9 eV for C_{14} and 1.0 eV for C_{15}). Meanwhile, the number of possible sp^2 isomers increases exponentially. Consequently, a full exploration of all topological isomers becomes computationally impossible, and thus, the careful selection of isomers to be explored is crucial. Our calculations revealed that polygonal rings other than pentagons and hexagons, such as quadrangles, heptagons, and octagons, always result in high formation energy. Thus, only the isomers

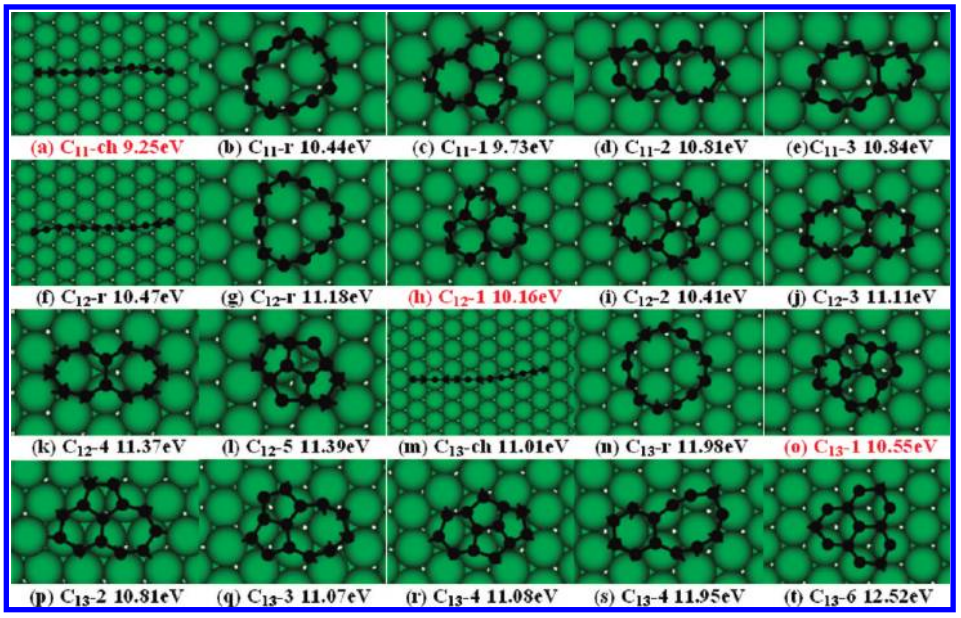

Figure 3. Structures and formation energies of some low energy C_{11}∼C_{13} isomers on a Ni (111) surface. "r" and "ch" in the notation C_N-r or C_N-ch stand for ring and chain, respectively. For each cluster size, the lowest-energy isomer is highlighted by red labels.

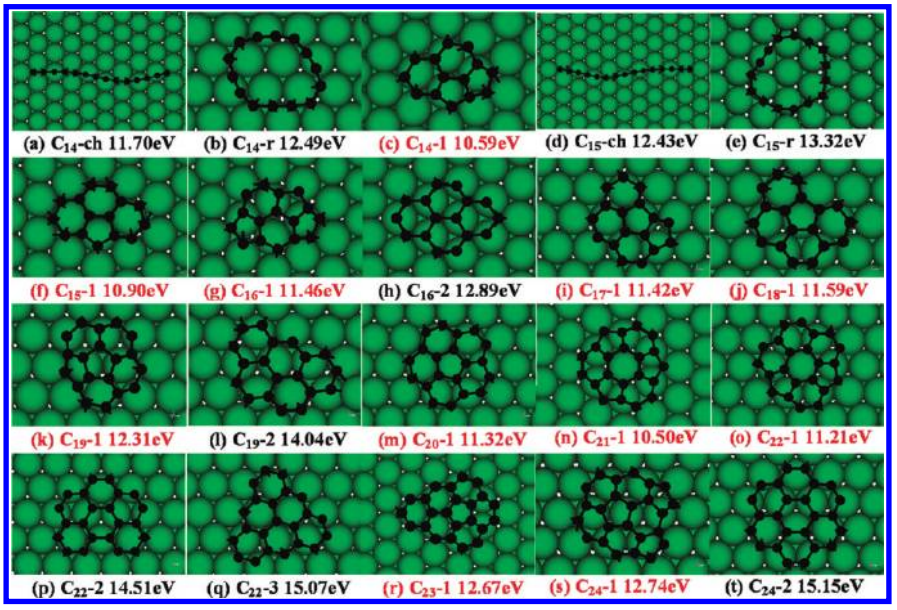

Figure 4. Structures and formation energies of some low energy C_{14}∼C_{24} isomers on a Ni (111) surface. Chains (a and d) and rings (b and e) of C_{14}∼C_{15}, and some isomers that contain only six-member-rings (h, l, p, q, and t) are shown. For each cluster size, the lowest-energy isomer is highlighted by red labels.

consisting of six-membered rings (6MRs) and five-membered rings (5MRs) have been considered here. For each size, we carefully selected at least ten isomers by giving high priority to those with less edge atoms (see discussion about the interaction between edge atoms and TM surfaces below). As representatives, the isomer structures explored for C_{14}, C_{19}, and C_{23} are summarized in Figure 6 and the Supporting Information S1 and S2, respectively.

Figure 4 displays the lowest-energy structures of Ni-supported C_N (N = 14−24) clusters and some of their important isomers. Interestingly, the most stable structures always contain one to three pentagons. The 6MR-only isomers are always energetically unfavorable with regard to the ground state ones. The ground state of C_{17} and C_{18} can be viewed as incomplete 2D core−shell structures with a central pentagon (Figure 4, panels i and j). As clusters grows bigger (N = 19−24), the core−shell configuration is closed (Figure 4, panels k, m, n, o, and r) and the central pentagon is replaced by a hexagon in the cases of C_{21}, C_{22} and C_{23} (Figure 4, panels n, o, and r). Although C_{24} has a high-symmetry core−shell isomer composed of seven hexagons (Figure 4t), its formation energy is higher than that of the ground state (Figure 4s) by 2.41 eV. This is further evidence of that the small hexagon-only islands are energetically unfavorable.

dx.doi.org/10.1021/jp2051454 |J. Phys. Chem. C 2011, 115, 17695–17703

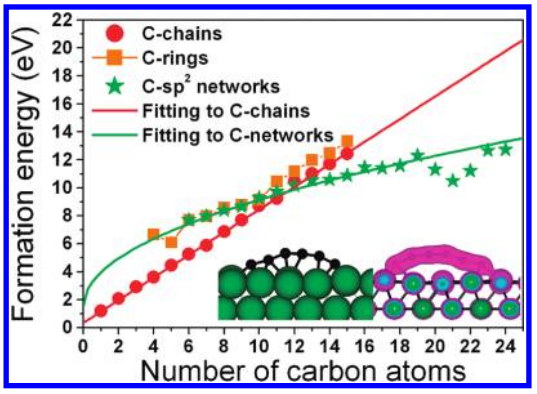

Figure 5. Formation energies of chains, rings, and most stable sp^2 networks on the Ni(111) surface versus the number of carbon atoms. The inserted figures show the atomic structure of a C chain with two ends tightly bound to the Ni(111) surface (left) and the charge density distribution on the cross section through the C chain (right). It can be seen that both end C atoms bind tightly to the metal surface.

DISCUSSION

Competition and Transition between Different Structural Patterns. Figure 5 shows the formation energies of chains, rings and the most stable sp^2 networks on a Ni(111) surface as a function of the number of C atoms. The order of formation energies is very different from that of C clusters in vacuum, where the ring configuration is the ground state in the size range of $10 < N < 20$ and bowl or fullerene structures becomes dominant in larger clusters (see details in the Supporting Information S3).[54,58] Within the entire size range of our calculations ($N \leq 24$), carbon chains on the Ni (111) surface are always found to be more stable than the ring configurations of the same size. The presence of the metal surface significantly stabilized the C clusters due to their interaction with the metal surface. For example, the formation energy of the most stable C_{20}@Ni(111) is more than 10 eV lower than that of a free C_{20} cluster (11.32 vs 22.61 eV) although the 20 C atoms are arranged in exact same configuration in both clusters (see Figure 4 and Figure S3).This can be understood in terms of the competition between the curvature energy of a ring and the end formation energy of a chain. In vacuum, each carbon chain has two freestanding end atoms with a very high formation energy of $E_e \sim 3.0$ eV/end (see the Supporting Information S3). On the other hand, a carbon ring, which can be viewed as a bent chain, that has no ends but carries extra curvature energy due to the deviation from perfect sp^1 hybridization. Intuitively, the curvature energy (E_c) of a ring is proportional to the inverse of ring diameter (D), $E_c \sim 1/D$. Consequently, in a vacuum, the ring structure becomes more and more stable with increasing cluster size and eventually dominates the ground state at $N = 10$. In contrast, on the Ni(111) surface, both ends of a carbon chain are bound tightly to the TM atoms and TM passivation significantly reduces the end formation energy more than 1 order of magnitude, from ~3.0 eV/end to ~0.2 eV/end (see the Supporting Information S3). Such a remarkable reduction of end formation energy stabilizes the chain configurations and thus the ring formation never becomes the ground state structure in the investigated C cluster size range.

As shown in Figure 5, as a 1D structure, the formation energies of the carbon chains can be fitted perfectly to a linear relationship. On the other hand, the formation energy of a 2D sp^2 island is mainly contributed to by the edge atoms. Hence the formation energy of a sp^2 aggregate can be fitted by

$$E_{sp^2} = \alpha^* N^{1/2} + \beta \quad (eV) \tag{2}$$

where $\alpha = 2.4$ eV and $\beta = 1.6$ eV. Here the second term β refers the intrinsic formation energy of a graphene island on the Ni(111) surface, i.e., $E_{sp2} = \beta$ at $N = 0$. As discussed above, the crossover between the 1D chains and the 2D sp^2 network occurs at $N = 12$, beyond which the energy difference between chain and sp^2 configurations becomes larger and larger (see Figure 5).

Nucleation Barrier (G^*) and Size of Nuclei (N^*) for Graphene Nucleation on the Ni(111) Surface. As stated above, their ground structures and their corresponding formation energies of Ni(111) supported C clusters can be classified into two categories: (i) one-dimensional (1D) C chains for $N < 12$, whose formation energy is nearly linear to N, and (ii) two-dimensional (2D) C networks/graphene islands for $N \geq 12$, which formation energy should be proportional to the number of edge atoms, $\sim N^{1/2}$. The linear tendency (i) can be clearly seen in the E vs N plot (Figure 6a), whereas the tendency (ii) is not that clear in the explored cluster size range ($N \leq 24$) because of the small size range of explored clusters.

According to the classical crystal growth theory, critical parameters regarding the graphene nucleation and growth, the size of nuclei, N^*, and the nucleation barrier, G^*, are determined by the maximum of the Gibbs free energy:

$$G(\mathrm{N}, \Delta\mu) = E(N) - N\Delta\mu \tag{3}$$

where $E(N)$ is the energy of the ground structure of cluster C_N and $\Delta\mu$ is the chemical potential drop from feedstock phase (the vapor phase of the VLS or VSS model[32−35]) to the graphene phase. Figure 6a shows the functions of G vs N at different $\Delta\mu$, one can clearly see the determination of (G^*, N^*) at every $\Delta\mu$.

Carefully calculated G^* vs $\Delta\mu$ and N^* vs $\Delta\mu$ are plotted in Figure 6b. It clearly shows an abrupt drop of N^* from ~12 to ~1 at $\Delta\mu \sim 0.8$ eV, which corresponds to the C_N clusters' ground structure transition from 1D to 2D at $N = 12$. From Figure 6a, one can see that the abrupt drop of size of nuclei was stemmed from the linear relationship of E vs N in the range of $N < 12$. In the range of $0.4 \text{ eV} < \Delta\mu < 0.8$ eV, N^* nearly maintains a constant number, the critical value of ground structure transition, $N^* \sim N_c = 12$ and the G^* drops linearly. That is because of the discontinuity of energy's first derivative at $N = 12$. The energy of linear chain can be fitted as $E \sim 0.81$ N eV. While, on the network side, the energy can be fitted as $E \sim 0.35$ N eV. The linear behavior difference results in a fact that maximum of the function $G(N)$ appears near $N = 12$ in a broad range of $0.35 \text{ eV} < \Delta\mu < 0.81$ eV and thus the N* is nearly a constant number in the range of $0.35 \text{ eV} < \Delta\mu < 0.81$ eV. It is worthwhile to note that, for $\Delta\mu < 0.2$ eV, the size of nuclei is out of the explored cluster range or $N^* > 24$. So we cannot predicate the exact nucleation barrier and the size of nuclei in that range correctly based on the presented calculation.

Strong Interaction between Edge C Atoms and the TM Surface. Figure 7 shows the structures and formation energies of twelve sp^2 network isomers of C_{14}. The formation energies of these isomers as function of the number of edge atoms (highlighted in red in Figure 7, panels a−l) are also plotted in the right graph of Figure 7. Recently, it was found that only the edge atoms of a graphene island interact strongly with the metal substrate.[59] Figure 7 shows correlation between the formation energy and

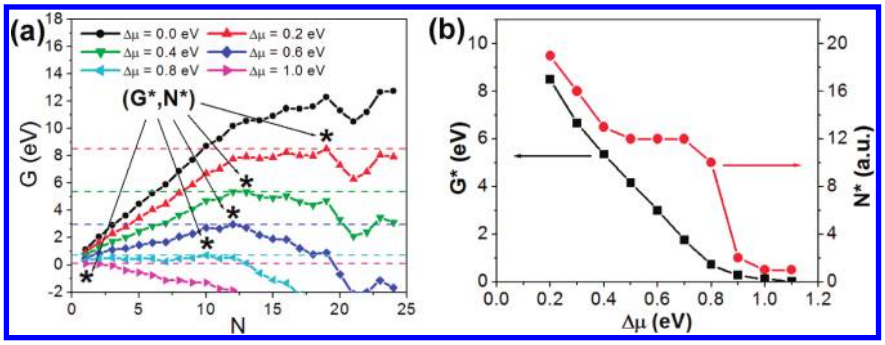

Figure 6. (a) Gibbs free energies, $G(N) = E(N) - N\Delta\mu$, of Ni(111) supported C clusters as a function of cluster size at $\Delta\mu$ = 0.0, 0.2, 0.4, 0.6, 0.8, and 1.0 eV, respectively. The maximum point (G^*, N^*) of the functions are marked by "*". (b) The calculated nucleation barrier, G^*, and size of nuclei, N^*, as a function of $\Delta\mu$.

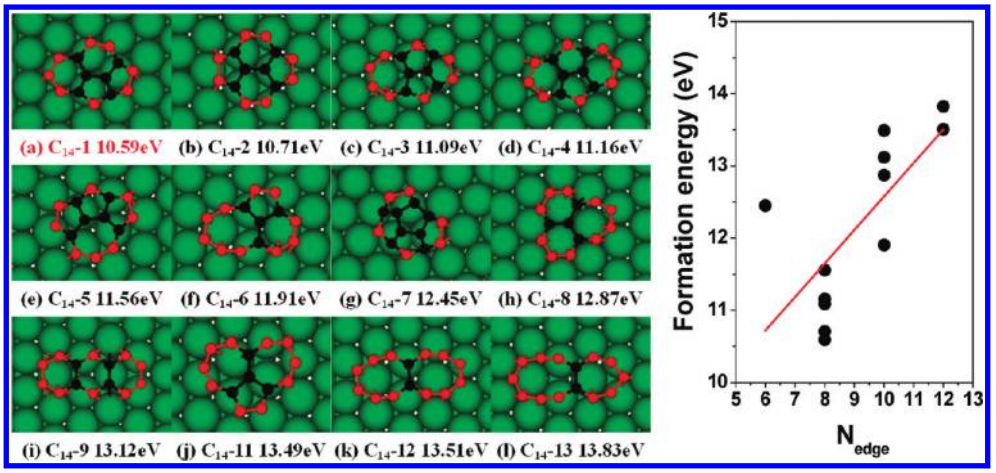

Figure 7. Optimized structures and formation energies of twelve sp^2 isomers of C_{14} supported on a Ni(111) surface (left) and their formation energies versus the number of edge atoms for all these isomers, N_{edge} (right). The C atoms with three neighbors are represented as black balls and the edge atoms are highlighted as red balls.

number of edge atoms. Each of the top five lowest-energy sp^2 networks (Figure 7, panels a−e) has eight edge atoms, whereas most other sp^2 isomers contain at least ten edge atoms. However, there is one exception that the structure of Figure 7g has only six edge atoms but a high formation energy. This isomer is composed of five 5MRs and is strongly curved upward. In other words, its high formation energy can be explained by the high curvature in its sp^2 network body. Detailed discussion on the competition between the edge formation energy and curvature energy will be given in the next subsection.

As shown in Figure 6, inclusion of large polygonal rings beyond hexagons, such as heptagons (Figure 7, panels c, e, h, j, and l), octagons (Figure 7, panels f and k). or nonagons (Figure 7l), into a sp^2 island always results in a remarkable increase in energy. Therefore we conclude that most low-energy sp^2 isomers should contain mainly pentagons and hexagons (see Figures 3, 4, 6).

Role of 5-membered-rings (5MRs) in the sp^2 Networks. As shown in Figures 3 and 4, all of the lowest-energy sp^2 isomers consist of one to three pentagons. The formation energy of a hexagon-only sp^2 aggregate is significantly greater than the most stable isomer (Figure 8a). Incorporating pentagons into an sp^2 network will curve the flat island up into a cap or bowl-like shape and therefore reduces its circumference length as well as the number of edge atoms. As shown above, the reduction of edge atoms lowers the edge formation energy of the graphene island but simultaneously builds up the curvature energy in the body of the island. Therefore, the optimal number of pentagons in the most stable sp^2 configuration is determined by the competition between the curvature energy and the edge formation energy. As shown in Figure 7g, the isomer formed by five pentagons possesses a high formation energy even though it has the smallest number of edge atoms among all the sp^2 isomers of C_{14} explored.

To further elucidate the correlation between the cap curvature and the formation energy, we have plotted the formation energies of C_{16} and C_{24} clusters as function of their height (the vertical distance between the topmost and the bottommost C atoms on the Ni (111) surface) in Figure 8b. On the Ni(111) surface, the 6MR-only sp^2 isomers (e.g., C_{16}-2 and C_{24}-2) are nearly flat. Thus they possess less curvature energy but have a longer circumference and consequently a higher edge formation energy. On the other hand, incorporating many pentagons ($N_5 > 3$) into a sp^2 network curves it up substantially (e.g., C_{16}-5 or C_{24}-5), and reduces its circumference length and number of edge atoms. The reduced edge formation energy is, however, compensated by the high curvature energy. Overall, as shown in Figure 7, incorporation of one to three pentagons into sp^2 networks is optimal to balance the curvature energy and the edge energy to achieve the most stable configuration (e.g., C_{16}-1 and C_{24}-1).

It is noteworthy that carbon aggregation with a few pentagons in the initial nucleation stage of graphene does not imply that the

dx.doi.org/10.1021/jp2051454 |J. Phys. Chem. C 2011, 115, 17695–17703

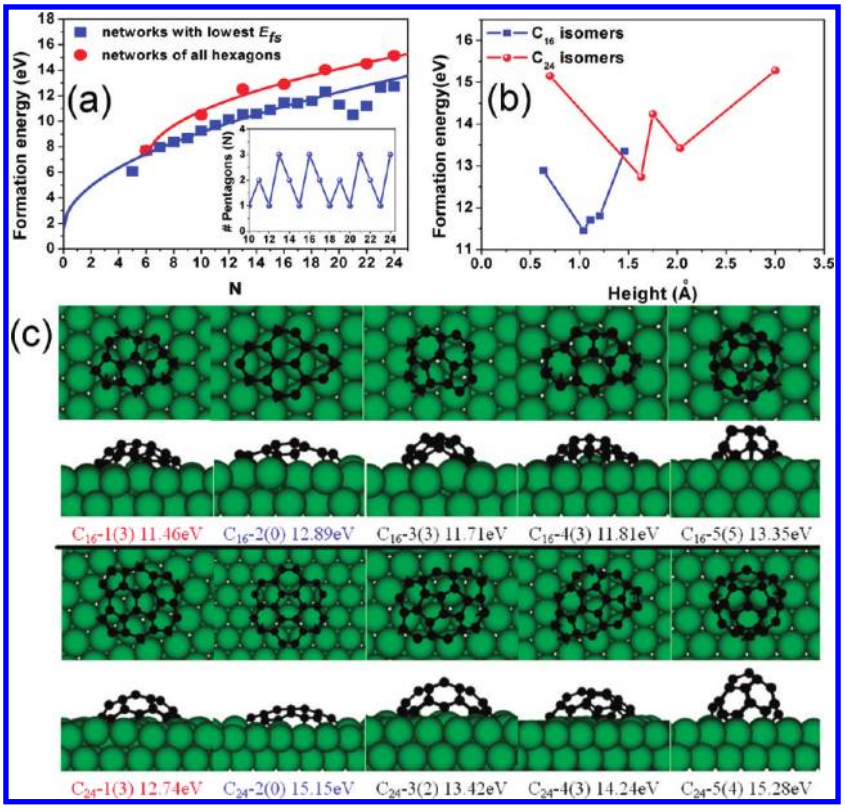

Figure 8. (a) Formation energies of the lowest-energy sp^2 aggregates, hexagon-only structures as a function of cluster size. The inserted graph is the number of pentagons in the lowest energy sp^2 island as a function of cluster size. (b) The formation energy as a function of cluster height for C_{16} and C_{24} clusters as shown in (c). (c) Top view and lateral view of C_{16} and C_{24} isomer structures. The number of pentagons for each configuration is shown in brackets.

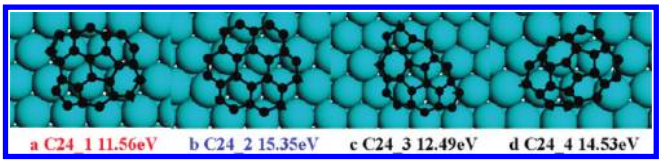

Figure 9. Four isomers and their formation energies of C_{24} on Ir(111) surface.

graphene grown would be highly defective because every nucleus may finally grow into a large graphene patch of up to a few hundreds μm. Moreover, since the 5MRs mainly exist in the nucleus region of graphene, finding the defective aggregate in CVD grown graphene might be used to identify the location of the initial nucleation site.

Graphene Islands on Other Metal Surfaces: the Low Energy Structures of the C_{24}@Ir(111). The result presented in this study is different from the intuition of graphene or graphene islands that both are hexagonal sp^2 networks: the former is infinite in size and the later is finite with a circumferential edge. Certainly, future experimental evidence are very importance to validate the presented result. Recently, Lacovig, P. et al. have addressed the dome-like graphene islands on Ir(111) surface.[40] They have shown that a graphene island is bonded to the Ir(111) substrate mainly through the strong interaction between edge C atoms and metal surface. They have proposed the dome-like graphene islands that contain only 6-membered-rings (hexagons). In previous study, because of the intuition of graphene island formation, only hexagonal sp^2 C networks were considered, which certainly excludes the formation of pentagons in graphene islands. Therefore, to show the analogy of various transition metals in graphene CVD growth, we explored 4 isomers of supported C_{24} clusters on Ir(111) surface (Figure 9). First, one can see that, on both metal surfaces, the C_{24} cluster has same ground structure, which contains 3 pentagons and 5 hexagons. Second, the energy difference between the 6-membered-ring only island and the ground state is very high for both: e.g., 2.41 and 2.97 eV for C_{24}@Ni(111) and C_{24}@Ir(111), respectively. So we are confident that every dome-like graphene islands observed in the previous study mostly contain one or a few pentagons.[40] The above results also showed that pentagons in small graphene islands on Ir(111) is also crucial and proves that the study of C_N@Ni(111) also shed lights on the role of many other metals in graphene CVD growth.

CONCLUSIONS

We have systematically studied the structural evolution of carbon clusters on the Ni(111) surface. Similar to the gas-phase carbon clusters, there is a structural transformation in the Ni-supported clusters. The most stable structural motif for the supported C_N cluster switches from 1D sp^1 chains to 2D sp^2 networks at a critical size of $N = 12$.

Our calculations also confirm that only edge C atoms of a graphene island interact strongly with the metal substrate. Most importantly, we found that incorporating few pentagonal rings into a small graphene patch is crucial for reducing its formation

dx.doi.org/10.1021/jp2051454 |J. Phys. Chem. C 2011, 115, 17695–17703

energy by reducing the number of edge atoms. Due to the larger number of edge atoms, sp^2 isomers containing only 6MRs are significantly less stable than the lowest-energy configurations with 5MRs.

Compared with on Ni and Ir, similar behaviors of C clusters were found. That means the law about graphene growth on Ni surface can be generalize to that on other transition metal surface. This study sheds light on the initial nucleation of graphene in CVD experiments. The present theoretical results will certainly guide experimental design to achieve high quality graphene on TM substrates.

Very recently, Kim et al. demonstrated the thermal CVD growth of nanographene on many different noncatalytic substrates, including semiconductors (e.g., silicon), insulators (e.g., silicon oxide), and transparent substrates (e.g., quartz).[60] It is apparent that these noncatalytic grown graphenes are much smaller in size and much lower in quality than those transition metal catalyzed ones. Although understanding the exact role of these noncatalytic surfaces in graphene growth requires further exploration which is beyond the scope of this work, one might guess that the growth of graphene on them is between that on transition metal surface and the free-standing C formation in vacuum (see the Supporting Information S3). In both cases, the structure of small C_N clusters ($N \approx 12$ on Ni(111) surface and $N \approx 10$ in vacuum) are dominated by sp C chain and a transition from sp C chain to sp^2 C network which has a few pentagons at a critical size. Therefore, it is expected that there is also a dominating size range for sp C chain and a transition from sp C chain to sp^2 C network transition in the initial nucleation stage of graphene on these substrates.

■ ASSOCIATED CONTENT

Supporting Information. Structures and formation energies of C_{19} and C_{23} isomers. The formation energies of carbon clusters in vacuum and most stable structures in sp^2 carbon aggregates. The formation energy linear fit and end formation energies of carbon chain on Ni(111) surfaces. This material is available free of charge via the Internet at http://pubs.acs.org.

■ AUTHOR INFORMATION

Corresponding Author

*E-mail: feng.ding@rice.edu; zhaojj@dlut.edu.cn.

Author Contributions

‖These authors contributed equally to this work.

■ ACKNOWLEDGMENT

This work was supported by Hong Kong Polytechnic University funds (A-PD1U; A-PH93; A-PJ50) and the Fundamental Research Funds for the Central Universities of China (No. DUT10ZD211).

■ REFERENCES

(1) Novoselov, K. S.; Geim, A. K.; Morozov, S. V.; Jiang, D.; Zhang, Y.; Dubonos, S. V.; Grigorieva, I. V.; Firsov, A. A. *Science* **2004**, *306*, 666.
(2) Geim, A. K.; Novoselov, K. S. *Nat. Mater.* **2007**, *6*, 183.
(3) Geim, A. K. *Science* **2009**, *324*, 1530.
(4) Frank, I. W.; Tanenbaum, D. M.; Zande, A. M. v. d.; McEuen, P. L. *J. Vac. Sci. Technol. B* **2007**, *25*, 2558.
(5) Lee, C.; Wei, X.; Kysar, J. W.; Hone, J. *Science* **2008**, *321*, 385.
(6) Balandin, A. A.; Ghosh, S.; Bao, W.; Calizo, I.; Teweldebrhan, D.; Miao, F.; Lau, C. N. *Nano Lett.* **2008**, *8*, 902.
(7) Wallace, P. R. *Phys. Rev.* **1947**, *71*, 622.
(8) Bostwick, A.; Ohta, T.; McChesney, J. L.; Seyller, T.; Horn, K.; Rotenberg, E. *Eur. Phys. J.-Spec. Top.* **2007**, *148*, 5.
(9) Son, Y.-W.; Cohen, M. L.; Louie, S. G. *Nature* **2006**, *444*, 347.
(10) Li, X.; Wang, X.; Zhang, L.; Lee, S.; Dai, H. *Science* **2008**, *319*, 1229.
(11) Young, A. F.; Kim, P. *Nat. Phys.* **2009**, *5*, 222.
(12) Novoselov, K. S.; Jiang, D.; Schedin, F.; Booth, T. J.; Khotkevich, V. V.; Morozov, S. V.; Geim, A. K. *Proc. Natl. Acad. Sci. USA.* **2005**, *102*, 10451.
(13) Ohta, T.; Bostwick, A.; Seyller, T.; Horn, K.; Rotenberg, E. *Science* **2006**, *313*, 951.
(14) Berger, C.; Song, Z.; Li, X.; Wu, X.; Brown, N.; Naud, C.; Mayou, D.; Li, T.; Hass, J.; Marchenkov, A. N.; Conrad, E. H.; First, P. N.; de Heer, W. A. *Science* **2006**, *312*, 1191.
(15) Sutter, P. *Nat. Mater.* **2009**, *8*, 171.
(16) Bostwick, A.; Ohta, T.; Seyller, T.; Horn, K.; Rotenberg, E. *Nat. Phys.* **2007**, *3*, 36.
(17) Stankovich, S.; Dikin, D. A.; Piner, R. D.; Kohlhaas, K. A.; Kleinhammes, A.; Jia, Y.; Wu, Y.; Nguyen, S. T.; Ruoff, R. S. *Carbon* **2007**, *45*, 1558.
(18) Choucair, M.; Thordarson, P.; Stride, J. A. *Nat. Nanotechnol.* **2009**, *4*, 30.
(19) Vaari, J.; Lahtinen, J.; Hautojärvi, P. *Catal. Lett.* **1997**, *44*, 43.
(20) Land, T. A.; Michely, T.; Behm, R. J.; Hemminger, J. C.; Comsa, G. *Surf. Sci.* **1992**, *264*, 261.
(21) Sutter, P. W.; Flege, J.-I.; Sutter, E. A. *Nat. Mater.* **2008**, *7*, 406.
(22) Coraux, J.; N'Diaye, A. T.; Busse, C.; Michely, T. *Nano Lett.* **2008**, *8*, 565.
(23) Pletikosić, I.; Kralj, M.; Pervan, P.; Brako, R.; Coraux, J.; N'Diaye, A. T.; Busse, C.; Michely, T. *Phys. Rev. Lett.* **2009**, *102*, 056808.
(24) Coraux, J.; N'Diaye, A. T.; Engler, M.; Busse, C.; Wall, D.; Buckanie, N.; Heringdorf, F.-J. M. z.; Gastel, R. v.; Poelsema, B.; Michely, T. *New J. Phys.* **2009**, *11*, 023006.
(25) Dedkov, Y. S.; Fonin, M.; Rüdiger, U.; Laubschat, C. *Phys. Rev. Lett.* **2008**, *100*, 107602.
(26) Grüneis, A.; Vyalikh, D. V. *Phys. Rev. B* **2008**, *77*, 193401.
(27) Reina, A.; Jia, X.; Ho, J.; Nezich, D.; Son, H.; Bulovic, V.; Dresselhaus, M. S.; Kong, J. *Nano Lett.* **2008**, *9*, 30.
(28) Starodub, E.; Maier, S.; Stass, I.; Bartelt, N. C.; Feibelman, P. J.; Salmeron, M.; McCarty, K. F. *Phys. Rev. B* **2009**, *80*, 235422.
(29) Marchini, S.; Günther, S.; Wintterlin, J. *Phys. Rev. B* **2007**, *76*, 075429.
(30) Cao, H.; Yu, Q.; Jauregui, L. A.; Tian, J.; Wu, W.; Liu, Z.; Jalilian, R.; Benjamin, D. K.; Jiang, Z.; Bao, J.; Pei, S. S.; Chen, Y. P. *Appl. Phys. Lett.* **2010**, *96*, 3.
(31) Lee, Y.; Bae, S.; Jang, H.; Jang, S.; Zhu, S.-E.; Sim, S. H.; Song, Y. I.; Hong, B. H.; Ahn, J.-H. *Nano Lett.* **2010**, *10*, 490.
(32) Gorbunov, A.; Jost, O.; Pompe, W.; Graff, A. *Carbon* **2002**, *40*, 113.
(33) Ding, F.; Bolton, K.; Rosén, A. *J. Phys. Chem. B* **2004**, *108*, 17369.
(34) Kolasinski, K. W. *Curr. Opin. Solid State Mater. Sci.* **2006**, *10*, 182.
(35) Takagi, D.; Kobayashi, Y.; Homma, Y. *J. Am. Chem. Soc.* **2009**, *131*, 6922.
(36) Grantab, R.; Shenoy, V. B.; Ruoff, R. S. *Science* **2010**, *330*, 946.
(37) Yazyev, O. V.; Louie, S. G. *Nat. Mater.* **2010**, *9*, 806.
(38) Loginova, E.; Bartelt, N. C.; Feibelman, P. J.; McCarty, K. F. *New J. Phys.* **2008**, *10*, 093026.
(39) Loginova, E.; Bartelt, N. C.; Feibelman, P. J.; McCarty, K. F. *New J. Phys.* **2009**, *11*, 063046.
(40) Lacovig, P.; Pozzo, M.; Alfè, D.; Vilmercati, P.; Baraldi, A.; Lizzit, S. *Phys. Rev. Lett.* **2009**, *103*, 166101.
(41) Chen, H.; Zhu, W.; Zhang, Z. *Phys. Rev. Lett.* **2010**, *104*, 186101.
(42) Saadi, S.; Abild-Pedersen, F.; Helveg, S.; Sehested, J.; Hinnemann, B.; Appel, C. C.; Nørskov, J. K. *J. Phys. Chem. C* **2010**, *114*, 11221.

(43) Amara, H.; Bichara, C.; Ducastelle, F. *Phys. Rev. B* **2006**, *73*, 113404.
(44) Karoui, S.; Amara, H.; Bichara, C.; Ducastelle, F. *ACS Nano* **2010**, *4*, 6114.
(45) Gao, J.; Yip, J.; Zhao, J.; Yakobson, B. I.; Ding, F. *J. Am. Chem. Soc.* **2011**, *133*, 5009.
(46) Kresse, G.; Furthmüller, J. *Phys. Rev. B* **1996**, *54*, 11169.
(47) Kresse, G.; Furthmüller, J. *Comput. Mater. Sci.* **1996**, *6*, 15.
(48) Perdew, J. P.; Chevary, J. A.; Vosko, S. H.; Jackson, K. A.; Pederson, M. R.; Singh, D. J.; Fiolhais, C. *Phys. Rev. B* **1992**, *46*, 6671.
(49) Vanderbilt, D. *Phys. Rev. B* **1990**, *41*, 7892.
(50) Laasonen, K.; Pasquarello, A.; Car, R.; Lee, C.; Vanderbilt, D. *Phys. Rev. B* **1993**, *47*, 10142.
(51) Murata, Y.; Petrova, V.; Kappes, B. B.; Ebnonnasir, A.; Petrov, I.; Xie, Y.-H.; Ciobanu, C. V.; Kodambaka, S. *ACS Nano* **2010**, *4*, 6509.
(52) Wintterlin, J.; Bocquet, M. L. *Surf. Sci.* **2009**, *603*, 1841.
(53) Ding, F.; Harutyunyan, A. R.; Yakobson, B. I. *Proc. Natl. Acad. Sci. USA.* **2009**, *106*, 2506.
(54) Jones, R. O. *J. Chem. Phys.* **1999**, *110*, 5189.
(55) Amara, H.; Roussel, J.-M.; Bichara, C.; Gaspard, J.-P.; Ducastelle, F. *Phys. Rev. B* **2009**, *79*, 014109.
(56) Moors, M.; Amara, H.; Visart de Bocarmé, T.; Bichara, C.; Ducastelle, F.; Kruse, N.; Charlier, J.-C. *ACS Nano* **2009**, *3*, 511.
(57) Page, A. J.; Irle, S.; Morokuma, K. *J. Phys. Chem. C* **2010**, *114*, 8206.
(58) Tománek, D.; Schluter, M. A. *Phys. Rev. Lett.* **1991**, *67*, 2331.
(59) Lacovig, P.; Pozzo, M.; Alfè, D.; Vilmercati, P.; Baraldi, A.; Lizzit, S. *Phys. Rev. Lett.* **2009**, *103*, 166101.
(60) Kim, K.-B.; Lee, C.-M.; Choi, J. *J. Phys. Chem. C* **2011**in press.